Available online at www.sciencedirect.com
ScienceDirect
Ceramics International 37 (2011) 303–311
CERAMICS INTERNATIONAL
www.elsevier.com/locate/ceramint

Engineering grain size and electrical properties of donor-doped barium titanate ceramics

Krisztian Niesz [a,*], Teyeb Ould-Ely [a], Hisashi Tsukamoto [b], Daniel E. Morse [a,**]

[a] Institute for Collaborative Biotechnologies, University of California, Santa Barbara, CA 93106-5100, USA
[b] Quallion LLC, 12744 San Fernando Road, Sylmar, CA 91342, USA

Received 19 June 2010; received in revised form 9 July 2010; accepted 28 August 2010
Available online 29 September 2010

Abstract

A semiconducting lanthanum-doped barium titanate ceramic has been fabricated for battery safety applications by simple means from nanoparticles prepared at room temperature by kinetically controlled vapor diffusion catalysis. The material, characterized by electron microscopy, X-ray diffraction and electrical measurements, exhibits a difficult to achieve combination of submicron grain size (~500 nm) and attractive electrical properties of room temperature resistivity below 100 Ω cm and a 12-fold increase in resistivity through the Curie temperature (positive thermal coefficient of resistivity, PTCR). Systematic investigation of sintering conditions revealed that a short period of heating at 1350 °C under air is necessary to suppress abnormal grain growth, while precise control of the cooling rate is needed to achieve the targeted electrical properties. Cooling must be sufficiently fast to avoid complete back-oxidation, yet slow enough to facilitate oxygen adsorption at the grain boundaries to produce the thin oxide layer apparently responsible for the observed PTCR.

Keywords: C. Electrical properties; Ceramics; Chemical synthesis; Crystal growth

1. Introduction

Although positive temperature coefficient of resistivity (PTCR) materials can be divided into four large groups (polymer composites, ceramic composites, V_2O_3-based compounds and $BaTiO_3$-based materials), sintered barium titanate-type ceramics have attracted superior attention as thermistors for a wide variety of applications [1–5]. A principal advantage of using $BaTiO_3$ stems from the fact that the sharp PTCR effect is not caused by volume expansion, which leads to extensive matrix cracking and irreproducibility, as characteristic of polymer and most typical ceramic composites, Furthermore, the semiconducting-insulator transition temperature (Curie temperature, T_C) can be precisely tuned to the required values through a wide temperature range by compositional changes. However, the problem of synthesizing such materials with sufficiently small grain size to permit, for example, device miniaturization while still maintaining the requisite electrical properties remains unsolved. Materials produced by conventional methods typically contain $BaTiO_3$ structures with relatively large grain sizes in the 10–100 micrometer regime, which is 2–3 orders of magnitude larger than required for miniaturization purposes. Although techniques such as spark plasma sintering and hot-pressing can suppress grain growth through sintering for shorter times or at lower temperatures to produce high density sintered ceramics with submicron grains, these technologies require high cost operation and maintenance [6,7]. High density ceramics with remarkably fine grain size (35 nm) can be also reached through a relatively simple two-step sintering process, in which the densification is grain boundary controlled and the final stage grain growth of barium titanate particles is sufficiently eliminated [8–10]. Although these materials can be used as piezoelectric ceramics, they lack the desired electrical properties required for PTCR applications. Furthermore, several groups have demonstrated a significant relationship between the grain size of donor-doped

* Corresponding author at: Institute for Collaborative Biotechnologies, University of California, Santa Barbara, 1209 Elings Hall, Santa Barbara, CA 93106-5100, USA. Tel.: +1 805 893 3416; fax: +1 805 893 8062.
** Corresponding author at: Institute for Collaborative Biotechnologies, University of California, Santa Barbara, 1209 Elings Hall, Santa Barbara, CA 93106-5100, USA. Tel.: +1 805 893 7442, fax: +1 805 893 8062.
E-mail addresses: krisztian.niesz@icb.ucsb.edu (K. Niesz), d_morse@lifesci.ucsb.edu (D.E. Morse).

0272-8842/$36.00
doi:10.1016/j.ceramint.2010.08.040

barium titanate ceramics and the overall electrical performance of the material [5,11–13]. Thus, if sintered at high temperature in air, the resulting ceramics consist of large grains and show high initial conductivity, whereas if the grain size is small (i.e., in the submicron regime), the final material exhibits high initial resistivity regardless of prior doping with electron donors. This behavior, the magnitude of which also is highly dependent on the donor dopant concentration, the presence of sintering aids, sintering temperature and the oxygen partial pressure during sintering, has been explained by the formation of an insulator grain boundary of adsorbed oxygen [14–16]. If the grain size is too small, the rapid growth of this grain boundary zone thus determines the overall electrical behavior of the material, causing it to behave as an insulator, that is typically white in color. In contrast, above a certain grain size, usually in the micrometer range, the material exhibits macroscopic semiconducting behavior and a grayish color. In addition to grain size and initial resistivity, the resistivity jump observed when the material is heated through the Curie temperature (T_C) also is highly dependent on sintering conditions generally exhibiting larger values when the sintering is done at high temperatures and in the presence of oxygen or air [5,17–23]. It thus remains a significant challenge to identify the delicate balance of synthesis of precursors, doping, sintering and post-annealing conditions required for applications that require a combination of small grain size, low initial resistivity and a significant PTCR [5].

For battery safety applications, we aim to fabricate a doped and sintered $BaTiO_3$ ceramic as a thin PTCR layer on the electrodes or current collector of lithium ion batteries as an internal safety device for protection against thermal runaway reactions from electrical short circuits (Scheme 1). Because this layer will tend to increase the total internal resistance of the battery and reduce its energy density, it is essential to make this ceramic as thin and as highly conductive in the initial state as possible, while still providing the protection of its PTCR. To achieve the optimal balance between safety and performance, we estimate that the target thickness of the ceramic layer should be ca. 10 μm or less, consisting of barium titanate particles of ca. 3 μm, each of which must contain submicron grains that are well fused through grain boundaries in order to prevent cancellation of the PTCR effect through parallel alignment of the grain

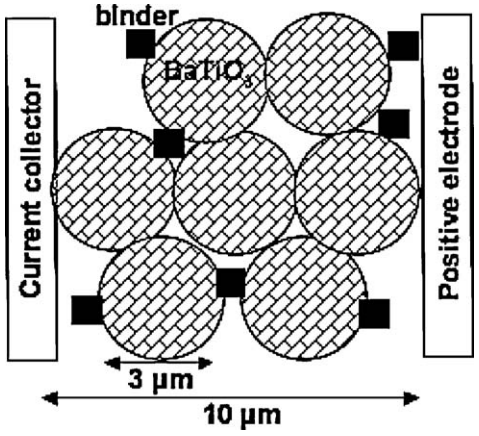

Scheme 1. Schematic representation of the proposed internal PTCR device.

polarities. The electrical parameters required for this application suggest that the ceramic layer must exhibit an initial resistivity of 100 Ω cm or less, with a PTCR increase in resistivity of >10-fold in the region between 110 °C and 150 °C.

We report here the results of our investigations aimed at achieving these specifications. As shown below, grain size in the final ceramic was engineered by control of the time and temperature of sintering, while the initial resistivity and the magnitude of the resistivity jump at T_C were further tuned by systematically varying the cooling rate.

2. Experimental procedure

2.1. Synthesis of barium titanate nanoparticles

Using uniform, nanosized crystalline particles in the sintering process is essential for the fabrication of high quality ceramic materials [24–26]. Donor-doped $BaTiO_3$ nanoparticles were synthesized using a modification of the method based on the room temperature, low-cost process described by Brutchey et al. [27,28]. This method results in high purity, highly crystalline $BaTiO_3$ particles with high surface area, particle size below 10 nm and spherical-like shape. Briefly, 25 ml of a single source bimetallic alkoxide ($BaTi(OCH_2CH(CH_3)OCH_3)_6$, 0.5 M, Gelest Inc.) was added to 5 ml of butanol containing 14.38 mg of lanthanum acetylacetonate ($La(AcAc)_3$, Aldrich) and then poured into a 3 neck round bottom flask filled with argon and connected through a glass bridge to another flask containing 40 ml of degassed 0.75 M HCl(aq) (Scheme 2). A dopant concentration of 0.17 at.% of La was targeted, as this concentration is below the critical donor dopant concentration (0.3 at.%) found to produce a grain size/electrical conductivity anomaly [13] and was found by our laboratory to deliver an optimal PTCR [27,28]. A gentle flow of Ar was used to drive the vapor from the water side toward the alkoxide precursor, while the latter was stirred at 300 RPM at room temperature until it went through the clearly visible gelation point and then reached the final state of suspension over the course of 24 h. Subsequently the product was purified by centrifugation and dispersion in butanol.

Post-doping was explored to improve the electrical properties of the final material. The influence of Mn ions is well described in the literature and known to increase the PTCR through the incorporation of Mn^{2+} ions into the Ti^{4+} lattice sites [29]. For this purpose, 1.4 mg of Mn(II) formate hydrate (Aldrich) was mixed with 2.3 g of the pre-synthesized $BaTiO_3$ nanopowder prior to sintering.

2.2. Sintering $BaTiO_3$ nanoparticles

For sintering, pellets with dimensions of 13 mm in diameter and 0.5 mm in thickness were prepared. Each pellet, containing 220 mg $BaTiO_3$ powder and 0.5 wt.% polyvinyl alcohol (PVA, Aldrich) as binder, was pressed at 100 MPa for 1 min under static vacuum. Sintering was conducted in a conventional high temperature muffle furnace (ThermoLyne 46100) under air. Sintering temperature and time were varied between 1100 °C

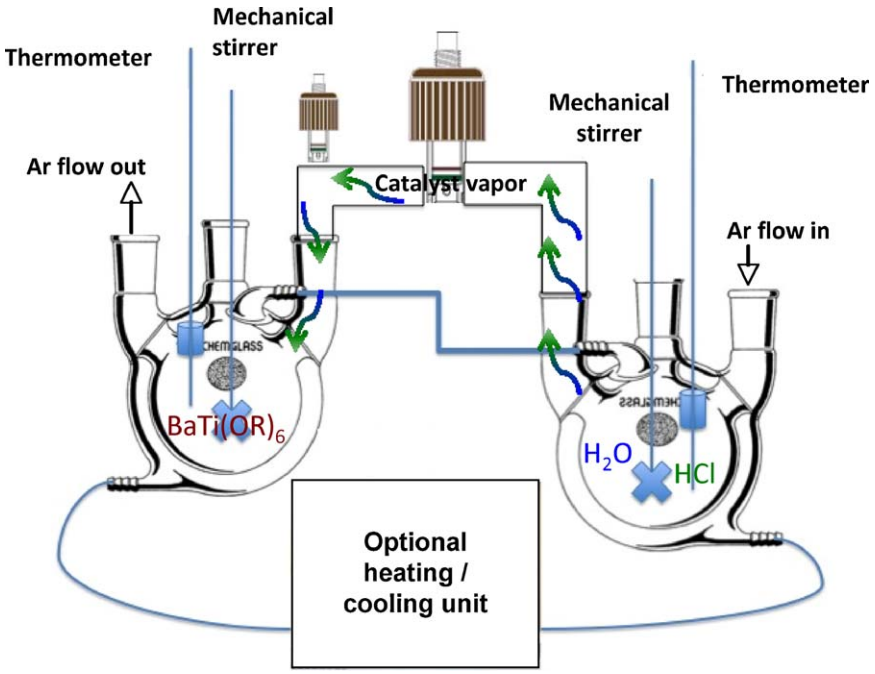

Scheme 2. Experimental setup for $BaTiO_3$ nanoparticle synthesis.

and 1420 °C and 1 min to several hours, respectively. Rates of heating and cooling rate were varied from 5 °C/min to ∼1000 °C/min. The maximum heating and cooling rates were reached when samples were placed directly into the furnace that had been pre-heated to the desired temperature or removed from the hot furnace and placed in a crucible previously cooled by liquid N_2, respectively. Lower cooling rates were achieved in the turned off furnace with or without ventilation. In those cases when high sintering temperatures were investigated in combination with high rates of heating, the samples first were calcined at 700 °C for 1 h prior to sintering to avoid cracking that otherwise would be caused by rapid gas evolution.

2.3. Characterization of the sintered ceramics samples

The lanthanum- and manganese contents of the samples were measured by Inductively Coupled Plasma Optical Emission Spectroscopy (ICP-OES) (Galbraith Laboratories). The size and morphology of the precursor $BaTiO_3$ nanocrystals were determined by transmission electron microscopy (TEM, FEI Technai G2 Sphera, 200 kV). Cubic to tetragonal phase transition during sintering was confirmed by XRD (Philips XPERT Powder Diffractometer, CuKα = 1.54 Å) primarily focusing on the asymmetric behavior and peak splitting of the (2 0 0) peak at $2\theta = 45^{o}$. Particle size was calculated from the broadening of the (1 1 0) peak with the Scherrer equation ($d = K * \lambda/\cos\theta * A$, where d is the particle size in nm, K is a shape factor (0.9), λ is the X-ray wavelength = 0.154 nm, θ is the Bragg angle and A is the FWHM in radians). The microstructural evolution of grains determined by the sintering conditions and the final grain sizes was monitored by SEM (Tescan Vega TS 5130MM). The electrical properties of the sintered ceramics, focusing on both the initial resistivity and the resistivity jump through the Curie temperature, were recorded on a Keithley 4200 Semiconductor Characterization System connected to Signaton 1160 Probe Station using the two-probe setup and a programmed heating stage. In/Ga (Aldrich) eutectic was used as electrode and brushed onto pellets of the samples. These samples were heated from room temperature to 200 °C and the change in resistance was monitored. Resistivity was calculated from the measured resistance values by taking into account the geometry and the dimensions of the pellets.

3. Results and discussion

3.1. Synthesis of La doped $BaTiO_3$ nanoparticles

$La_xBa_{1-x}TiO_3$ nanoparticles were prepared by combining continuous stirring with the kinetically controlled vapor diffusion method reported earlier [27,28]. The modified process, using 25 ml of the alkoxide precursor molecule, yielded, after drying, 3 g of high quality, phase pure $BaTiO_3$ nanocrystals in a powder form, representing quantitative yield, as shown in Fig. 1. We found that stirring of the precursor solution was necessary to produce multiple gram quantities of the $BaTiO_3$ nanocrystals in high yield and with high crystallinity. If not stirred, the quality of the product was found to decline rapidly with increased volume rapidly because of the formation of a dense layer of highly viscous gel on the surface of the solution, preventing further diffusion of water vapor into the bulk solution. Under these conditions the final size of the nanocrystals were significantly larger (8.6 nm and 8.2 nm by TEM and XRD, respectively) than 5.5 nm as had been observed for this synthesis method operated at the milligram scale [27,28]. This difference in size may be the result of the increased reaction rate and the resulting acceleration of crystal

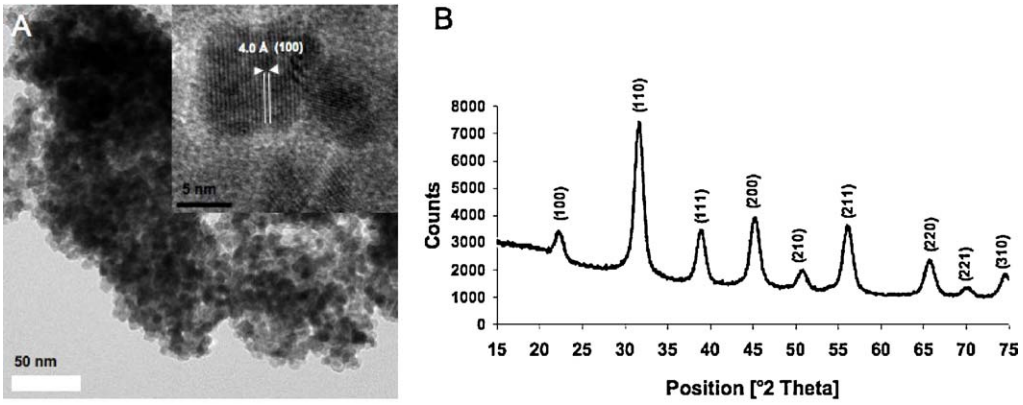

Fig. 1. (a) TEM image of the La doped $BaTiO_3$ nanoparticles (inset shows a representative high resolution TEM image on a randomly selected area from the same sample); (b) XRD of the La doped $BaTiO_3$ nanoparticles showing the characteristic diffraction peaks.

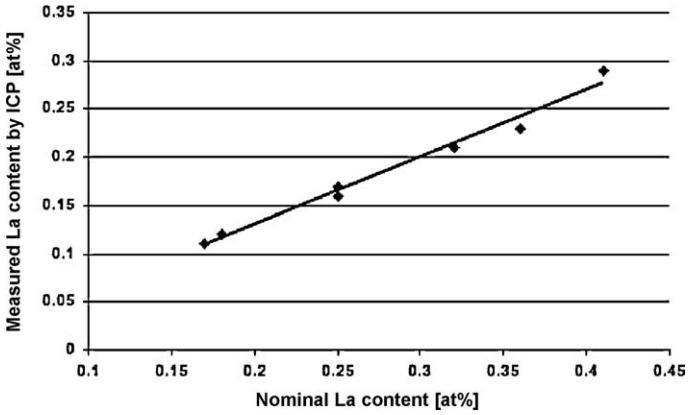

Fig. 2. Calibration curve for content of La dopant in $BaTiO_3$ ceramics as measured by ICP, shown as a function of nominal input values during synthesis.

growth caused by stirring the reaction mixture during synthesis. Moreover the as-prepared La doped $BaTiO_3$ nanoparticles are single crystalline, as shown in the higher resolution TEM images. The lattice fringes observed (4 Å) agree well with the separation of (1 0 0) planes. An experimental calibration based on ICP-OES measurements was used to aim at $x = 0.17$ at.% La content in the preparation of donor-doped $La_xBa_{1-x}TiO_3$ (Fig. 2). The Mn content of the post-doped samples was 0.09 at.% as measured by ICP.

3.2. Sintering temperature and time dependency

We first aimed to determine the sintering conditions required to produce the targeted submicron grain size desired for the internal PTCR layer application (cf. Scheme 1). Systematic investigation of sintering temperature and time led to the following observations. Sintering donor-doped $BaTiO_3$ pellets at 1350 °C for 4 h under air resulted in large heterodisperse grains (2–50 μm), orders of magnitude larger than required,

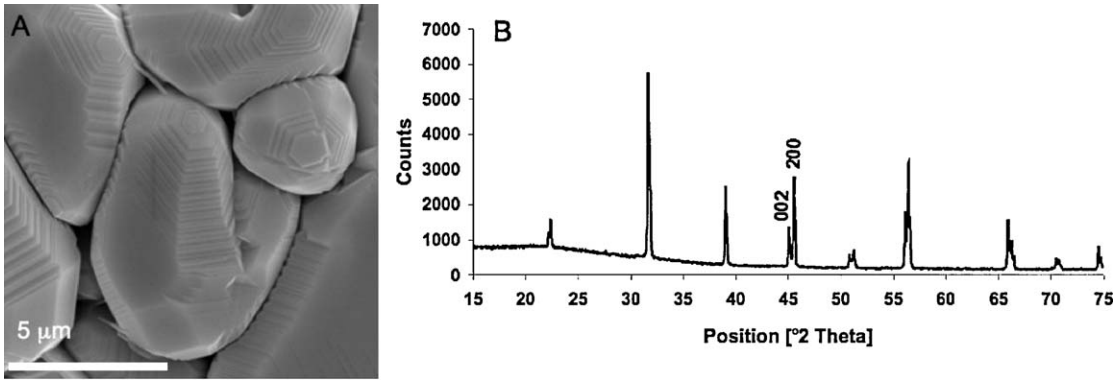

Fig. 3. (a) SEM image and (b) XRD of large polygonal grains obtained by sintering La doped $BaTiO_3$ pellets at 1350 °C for 4 h under air.

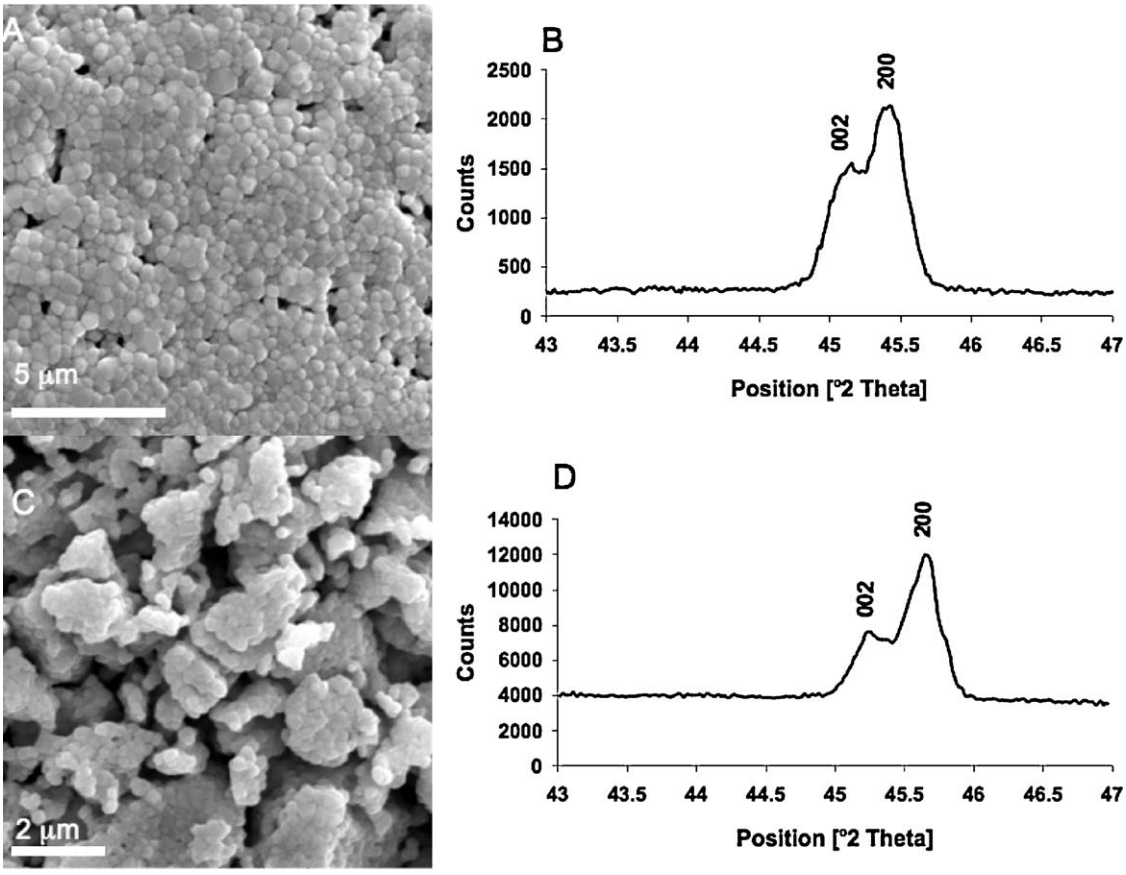

Fig. 4. (a) SEM image and (b) XRD data of La doped $BaTiO_3$ pellets after sintering at 1350 °C for 2 min followed by quick cooling; (c) SEM image and (d) XRD data of La doped $BaTiO_3$ pellets after sintering at 1200 °C for 30 min followed by cooling with 5 °C/min rate.

with irregular polygonal shapes (Fig. 3a). In this case, the sintering temperature exceeded the eutectic temperature (∼1320 °C), allowing the system to enter the abnormal grain growth regime, which is driven by the presence of a liquid phase and surface energy anisotropy [30]. In this very high temperature sintering, the particles grow out from the liquid phase by dissolution and re-crystallization on pre-formed nuclei, usually twin lamellae, resulting in a heterodisperse system containing a mixture of large grains embedded in a fine matrix of smaller particles [31]. We observed that the boundary facets of grains larger than 2 μm formed by this process often reveal valley-hill type facets that can be attributed to face reconstruction, as well as a step growth mechanism known to be another consequence of the liquid phase sintering process [32,33]. The cubic to tetragonal phase transition was demonstrated by XRD, which clearly shows the (0 0 2)/

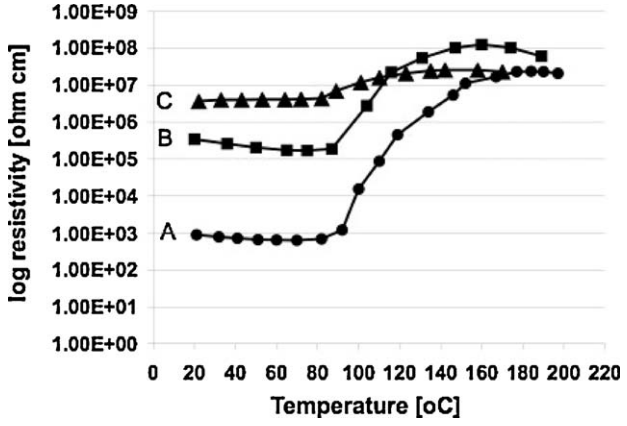

Fig. 5. Resistivity as a function of temperature exhibited by pellets of La doped $BaTiO_3$ ceramics produced by sintering and cooling in air under the following conditions: (a) 1350 °C for 4 h followed by cooling at 5 °C/min; (b) 1200 °C for 30 min followed by cooling at 5 °C/min; and (c) 1350 °C for 2 min, followed by removal from the furnace and cooling in air.

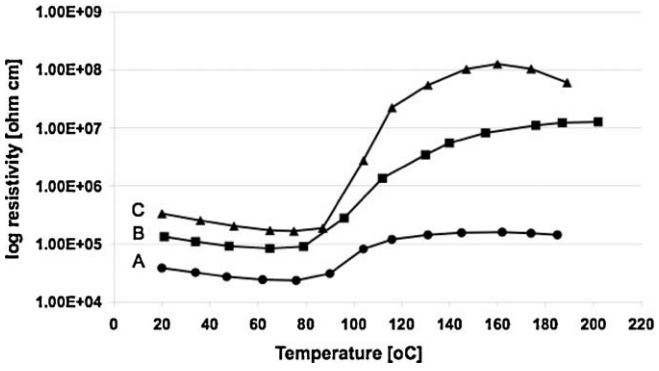

Fig. 6. Cooling rate dependency of electrical properties (resistivity vs. temperature) of La doped $BaTiO_3$ pellets after sintering at 1200 °C for 30 min; (a) rapid cooling on a liquid N_2 cooled surface, (b) cooling in a turned off furnace with ventilation, and (c) slow cooling with 5 °C/min rate.

(2 0 0) peak splitting at $2\theta = 45^\circ$ (Fig. 3b). Despite the abnormal grain growth (AGG) that occurs at high temperatures, we found that the size of the final grains can be kept in the required submicron regime by sintering the samples at 1350 °C only for a short period of time. An alternative strategy would be to maintain the sintering temperature below the eutectic, although the presence of microstructures containing {1 1 1} twins can often initiate AGG leading to large and heterodisperse grains under such conditions [34,35].

We have mapped the influence of sintering temperature and time on grain size and morphology, identifying different processing paths that can be used to reach the targeted size range; these include: (a) sintering at 1350 °C for 2 min only followed by rapid removal of the sample and cooling under air; and (b) sintering at 1200 °C for 30 min followed by cooling at a normal rate of 5 °C/min under air (Fig. 4). Although the splitting of the (2 0 0) diffraction peak is not clear in these cases, XRD investigations show the presence of an asymmetric peak at $2\theta = 45^\circ$ suggesting that these sintered samples are in fact in the tetragonal phase. The less prominent nature of the (2 0 0) peak splitting is related to the small grain size, ~200–400 nm. When sintering temperatures were higher than 1350 °C (e.g. 1420 °C, not shown), or sintering times longer than 2 min were used at 1350 °C, the resulting products contained large grains >10 micrometers in size, evidence of extremely fast crystal growth. Microscopic studies in conjunction with resistivity measurements showed a clear correlation, in good agreement with results previously reported by others, that the electrical properties of the ceramics are highly governed by the final size of the individual grains (among other factors), and that these are determined in large part by the sintering process [5]. Our samples formed under the conditions described above to yield grain size in the 200–

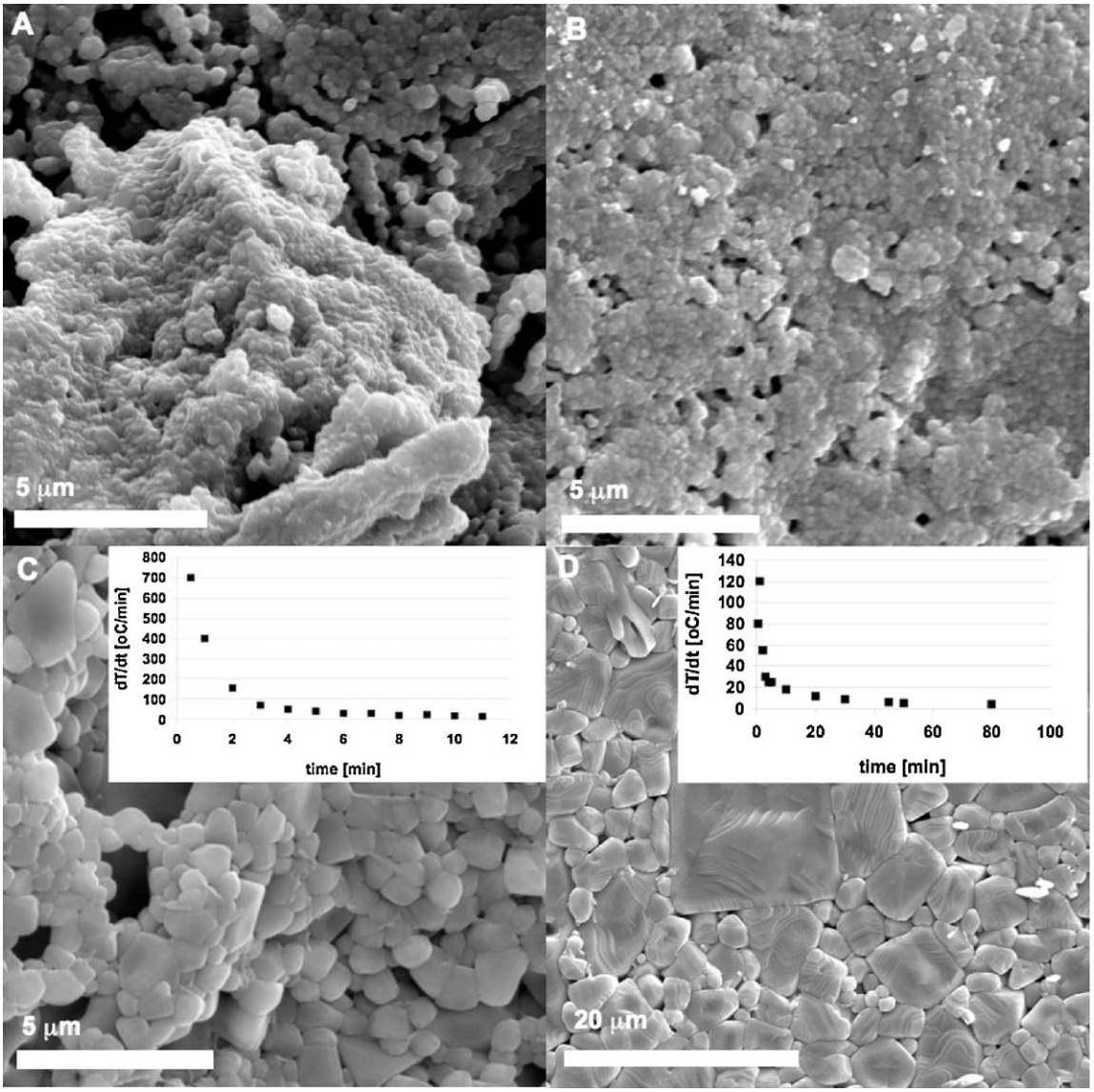

Fig. 7. SEM images of La doped $BaTiO_3$ ceramic pellets after sintering at 1350 °C for 2 min followed by different cooling processes. The cooling rates are shown as insets when measured. (a) Rapid cooling on a liquid N_2 cooled surface; (b) removal of the sample from the furnace and allowing it to cool in air; (c) cooling in a turned off furnace under ventilation; and (d) slowest cooling in a turned off furnace without ventilation.

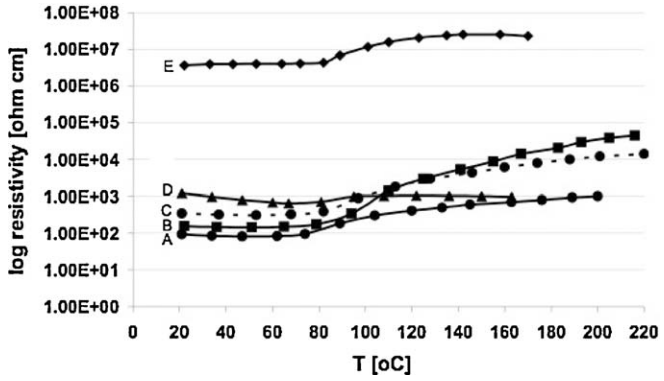

Fig. 8. Cooling rate dependency of electrical properties (resistivity vs. temperature) of La doped $BaTiO_3$ ceramic pellets after sintering at 1350 °C for 2 min followed by; (a) cooling in a turned off furnace under ventilation; (b) cooling in a turned off furnace without ventilation; (c) cooling in a turned off furnace under ventilation [sample post-doped with 0.09 at.% Mn]; (d) cooling on a liquid N_2 cooled surface; and (e) cooling by removal of the sample from the furnace and allowing it to cool in air.

400 nm range showed prohibitively high initial resistivity, up to the range of 10^5–10^6 Ω cm, and a resistivity jump of 7.6×10^2 and 7.0, depending on the sintering protocol (Fig. 5; curves b and c). These electrical properties can be explained by the large relative thickness of the oxidized layer around the core of each grain, called the grain boundary zone, indicative of significant back-oxidation of the samples [5,11]. The grain boundary layer is formed from adsorbed oxygen during cooling under air. If the grains are too small, then the sample can be completely re-oxidized, greatly reducing its conductivity. On the other hand, if the grains are large enough (2–50 μm), which is the case when high sintering temperature is paired with sufficiently long sintering time, then the oxidized layer can be relatively thin compared to the entire grain dimension; in the example shown in Fig. 5 (curve a), the material behaves as a reasonably good conductor, with an initial resistivity of 8.9×10^2 Ω cm and a significant 3.8×10^4-fold resistivity jump through T_C. These findings are in good agreement with the well-known consequence of defect chemistry that it is impossible to produce semiconducting donor-doped $BaTiO_3$ ceramics through solid-state growth when sintering under air, but that this can be accomplished by AGG [11]. Thus, it is extremely challenging to produce semiconducting barium titanate sintered ceramics with small, submicron grain size, low room temperature resistivity and significant PTCR behavior, all of which would be useful and required for applications in battery safety. When simply sintering samples at relatively lower temperatures or for shorter periods of time to keep the grain size small, the growth of the grain boundary layer of oxygen defeats all efforts to obtain significantly low initial resistivity. This led us to investigate the important influence of the cooling rate.

3.3. Cooling rate dependency

Our investigations showed that the cooling rate plays a significant role in defining the overall electric behavior of the doped $BaTiO_3$ sintered ceramics. XRD characterization of the samples discussed in the following section proves that all show the phase transition from cubic to tetragonal expected as a consequence of high temperature sintering (data not shown). Samples sintered at 1200 °C under air, forming ceramics through a solid state grow mechanism, exhibited a simple relationship between the cooling rate and final electrical properties. In these cases, no significant differences were observed in final grain size as a function of cooling rate. Both the initial resistivity and the PTCR value were found to decrease with increased cooling rate; initial resistivity declined from 3.3×10^5 Ω cm to 3.8×10^4 Ω cm, while the magnitude of the PTCR jump declined from 7.6×10^2 to 7.0, respectively (Fig. 6; curves a–c). These observations can be explained by the progressively smaller amounts of adsorbed oxygen and progressively less complete back-oxidation with progressively more rapid cooling. Although the size of the grains perfectly match the range targeted for the battery safety application (cf. Scheme 1 and Fig. 4c), the electrical performance of these samples still did not meet requirements. However, when ceramics were prepared by heating briefly to 1350 °C and then cooling under different conditions, very different results were obtained (Figs. 7 and 8). We found it essential to sinter at the high temperature for a very short period of time and then quickly initiate cooling in order to quench grain growth and avoid the production of larger grains. Representative SEM images of the ceramics produced under such conditions are illustrated as a function of cooling conditions in Fig. 7. The highest cooling rate was reached by quickly removing the samples from the hot furnace and placing them onto liquid N_2 cooled surfaces. This process resulted in small ceramic grains (~300 nm; cf. Fig. 7a) with an initial resistivity of 1.2×10^3 Ω cm and an insignificant PTCR jump (Fig. 8; curve d). We conclude that the extremely rapid cooling prevented any significant back-oxidation at the grain boundaries; thus, although little insulation at these boundaries occurred to reduce the initial conductivity, there also was insufficient oxygen adsorption at the grain boundaries for a strong PTCR effect. Thus, we concluded, a delicate balance had to be found. Decreasing the cooling rate by simply turning off the furnace resulted in a sample with room temperature resistivity of 1.6×10^2 Ω cm and a 300-fold resistivity jump when heated through the T_C (Fig. 8; curve b). However, during this very slow and relatively uncontrolled cooling, abnormal grain growth occurred to produce sizes as large as 10 μm (cf. Fig. 7d). The cooling rate measure under those conditions began at 120 °C/min and gradually decreased to 5 °C/min over the period of 1 h. By further increasing the cooling rate to an intermediate level, we found that we can produce a ceramic consisting of grains with submicron size (as shown in Fig. 7c) exhibiting the desired electrical characteristics of a low initial resistivity of 9.4×10^1 Ω cm and a significant, 12-fold jump in resistivity through the Curie temperature (Fig. 8; curve a). We thus were able to tune the processing conditions of sintering and cooling to retain the targeted grain size and low initial resistivity while building a sufficient layer of adsorbed oxygen required for a useful PTCR potentially practical for industrial applications. Note that in this case, because of the applied ventilation, the cooling rate started at a significantly higher value (700 °C/min)

Table 1
Summary of grain sizes and electrical properties of the $BaTiO_3$ ceramics as a function of processing conditions.

Sample preparation[a]	Grain size[b] (μm)	Initial resistivity (Ω cm)	PTCR through T_C (R_{max}/R_{min})
Sintered at 1350 °C for 4 h followed by slow cooling at 5 °C/min	~2–50 10	8.9×10^2	3.8×10^4
Sintered at 1350 °C for 2 min followed by cooling in a turned off furnace without ventilation	~1.0–15.7 2.3	1.6×10^2	3.0×10^2
Sintered at 1350 °C for 2 min followed by cooling in a turned off furnace under ventilation	~0.4–1.7 0.5	9.4×10^1	1.2×10^1
Post-doped with 0.09 at.% Mn and sintered at 1350 °C for 2 min followed by cooling in a turned off furnace under ventilation	~0.4–1.7 0.5	3.45×10^2	4.4×10^1
Sintered at 1350 °C for 2 min followed by cooling by removal from the furnace	~0.3–0.9 0.4	3.7×10^6	7.0
Sintered at 1350 °C for 2 min followed by rapid cooling on a liquid N_2 cooled surface	~0.3	1.2×10^3	N/A
Sintered at 1200 °C for 30 min followed by slow cooling at 5 °C/min	~0.2	3.3×10^5	7.6×10^2
Sintered at 1200 °C for 30 min followed by cooling in a turned off furnace under ventilation	~0.2	1.3×10^5	1.5×10^2
Sintered at 1200 °C for 30 min followed by rapid cooling on a liquid N_2 cooled surface	~0.2	3.8×10^4	7.0

a All sintering was conducted in air.

b The underlined grain sizes represent the most frequently measured (SEM) values in each sample.

and decreased quickly. Post-doping the $La_xBa_{1-x}TiO_3$ sample with 0.09 at.% Mn increased the PTCR jump by nearly 4-fold (from 12 to 45), but this dopant also increased the initial resistivity to 3.45×10^2 Ω cm, which is above the estimated 100 Ω cm limit for practicality (Fig. 8; curve c).

The effects of processing conditions on $BaTiO_3$ ceramic grain size, initial resistivity and PTCR are summarized in Table 1. These results, we believe, are helpful in understanding the complex interactions of sintering conditions on the grain size, composition and electrical properties of donor-doped $BaTiO_3$ ceramics, and thus can be used in designing custom materials for battery safety applications. They show that it is possible to engineer the grain size and electrical properties of sintered ceramics in tandem by simple means.

4. Conclusions

We have followed a simple strategy to fulfill the requirements of submicron grain size, low initial resistivity and significant PTCR of donor-doped $BaTiO_3$ ceramics by first tuning the grain size through systematic optimization of sintering temperature and time. Mapping the grain size vs. sintering conditions showed us two regimes resulting in samples with sufficiently small, submicron grains with tetragonal crystal phase. Sintering the initial high quality nanocrystalline powders below the eutectic, at 1100–1200 °C for 30 min under air at 5 °C/min heating and cooling rates produced ceramics with grain sizes around 200 nm. A second processing path to reach similarly small dimensions includes calcination of the sample at 700 °C followed by rapid heating to 1350 °C and fast cooling after 1–2 min annealing time. In this case, although briefly above the eutectic, rapid cooling quenches the liquid phase sintering and allows us to avoid the formation of larger grains. In all other cases we investigated, sintering at $T > 1350$ °C for longer than 2 min inevitably produced large polygonal grains as a result of abnormal grain growth.

With sintering conditions optimized to produce submicron grains as described above, we then tuned the electrical properties of the ceramics by investigating their cooling rate dependency. The desired combination of grain size and electrical properties was obtained with a rapid initial cooling rate followed by slower cooling. The resulting ceramic exhibits the desired submicron grain size, good semiconductor behavior (low initial resistivity) and a significant increase in resistivity when heated above T_C as required for the targeted battery safety application.

We plan to extend these investigations with measurements of the electrical behavior of single grains and grain boundaries by conductance atomic force microscopy to help us better understand and predict the electrical properties of these and related sintered ceramics.

Acknowledgments

This work was supported in major part by contracts from the Power and Energy Division, of the U.S. Army's Communications-Electronics Research, Development and Engineering Center (CERDEC), and secondarily by grants from the U.S. Army Research Office through grant DAAD19-03-D-0004 to the Institute for Collaborative Biotechnologies and the U.S. Dept. of Energy (DEFG03-02ER46006). We thank Dr. E.J. Plichta, Chief of the Power Division at CERDEC and M. Hendrickson, Chief Engineer at CERDEC, for their vision and

support, and Prof. Michael Doherty for his insights into the elusive subtleties of crystal growth mechanisms.

References

[1] D.W. Richerson, Modern Ceramic Engineering: Properties, Processing, and Use in Design, 2nd edn., Marcel Dekker, Inc., New York, NY, 1992

[2] J. Nowotny, M. Rekas, Dielectric ceramic materials based on alkaline earth titanates, Key Eng. Mater. 66/67 (1992) 45–143.

[3] S. Chatterjee, H.S. Maiti, A novel method of doping PTC thermistor sensor elements during sintering through diffusion by vapour phase, Mater. Chem. Phys. 67 (2001) 294–297.

[4] M. Wegmann, R. Bronnimann, F. Clemens, T. Graule, Barium titanate-based PTCR thermistor fibers: processing and properties, Sens. Actuators A: Phys. 135 (2) (2007) 394–404.

[5] B. Huybrechts, K. Ishizaki, M. Takata, The positive temperature coefficient of resistivity in barium titanate, J. Mater. Sci. 30 (1995) 2463–2474.

[6] M.B. Park, N.H. Cho, C.D. Kim, S.K. Lee, Phase transition and physical characteristics of nanograined $BaTiO_3$ ceramics synthesized from surface-coated nanopowders, J. Am. Ceram. Soc. 87 (3) (2004) 510–512.

[7] T. Takeuchi, M. Tabuchi, H. Kageyama, Y. Suyama, Preparation of dense batio$_3$ ceramics with submicron grains by spark plasma sintering, J. Am. Ceram. Soc. 82 (4) (1999) 939–943.

[8] I.-W. Chen, X.-H. Wang, Sintering dense nanocrystalline ceramics without final-stage grain growth, Nature 404 (2000) 168–171.

[9] X.-H. Wang, X.-Y. Deng, H.-L. Bai, H. Zhou, W.-G. Qu, L.-T. Li, I.-W. Chen, Two-step sintering of ceramics with constant grain-size, II: $BaTiO_3$ and Ni–Cu–Zn ferrite, J. Am. Ceram. Soc. 89 (2) (2006) 438–443.

[10] T. Karaki, K. Yan, M. Adachi, Barium titanate piezoelectric ceramics manufactured by two-step sintering, Jpn. J. Appl. Phys. 46 (2007) 7035–7038.

[11] J. Daniels, K.H. Hardtle, R. Wernicke, The PTC effect of barium titanate, Phillips Tech. Rev. 38 (1978) 73–82.

[12] A.F. Shimanskij, M. Drofenik, D. Kolar, Subsolidus grain growth in donor doped barium titanate, J. Mater. Sci. 29 (1994) 6301–6305.

[13] C.J. Peng, H.Y. Lu, Compensation effect in semiconducting barium titanate, J. Am. Ceram. Soc. 71 (1) (1988) 44–46.

[14] M. Drofenik, Oxygen partial pressure and grain growth in donor-doped $BaTiO_3$, J. Am. Ceram. Soc. 70 (5) (1987) 311–314.

[15] S. Urek, M. Drofenik, D. Makovec, Sintering and properties of highly donor-doped barium titanate ceramics, J. Mater. Sci. 35 (2000) 895–901.

[16] I. Zajc, M. Drofenik, Semiconducting $BaTiO_3$ ceramic prepared by low temperature liquid phase sintering, J. Mater. Res. 13 (1998) 660–664.

[17] W. Heywang, Resistivity anomaly in doped barium titanate, J. Am. Ceram. Soc. 47 (10) (1964) 484–490.

[18] G.H. Jonker, Some aspects of semiconducting barium titanate, Solid State Electron. 7 (1964) 895–903.

[19] M. Kubawara, Effect of microstructure on the PTCR effect in semiconducting barium titanate ceramics, J. Am. Ceram. Soc. 64 (11) (1981) 639–644.

[20] R.D. Roseman, N. Mukherjee, PTCR effect in $BaTiO_3$: structural aspects and grain boundary potentials, J. Electroceram. 10 (2003) 117–135.

[21] G. Lewis, C. Catlow, R. Casselton, PTCR effect in $BaTiO_3$, J. Am. Ceram. Soc. 68 (10) (1985) 555–558.

[22] A.B. Alles, V.L. Burdick, Grain boundary oxidation in PTCR barium titanate thermistors, J. Am. Ceram. Soc. 76 (2) (1993) 401–408.

[23] Y.-C. Chen, Annealing effects of semiconducting barium-titanate thermister, J. Marer. Sci. Technol. 15 (4) (2007) 307–314.

[24] H.L. Hsieh, T.T. Fang, Effect of green states on sintering behavior and microstructural evolution of high-purity barium titanate, J. Am. Ceram. Soc. 73 (6) (1990) 1566–1573.

[25] M. Drofenik, Initial morphology and grain growth in donor-doped barium titanate, J. Am. Ceram. Soc. 75 (9) (1992) 2383–2389.

[26] D. Segal, Chemical synthesis of ceramic materials, J. Mat. Chem. 7 (1997) 1297–1305.

[27] R.L. Brutchey, G. Cheng, Q. Gu, D.E. Morse, Positive temperature coefficient of resistivity in donor-doped $BaTiO_3$ ceramics derived from nanocrystals synthesized at low temperature, Adv. Mater. 20 (2008) 1029–1033.

[28] R.L. Brutchey, D.E. Morse, Template-free, low temperature synthesis of crystalline barium titanate nanoparticles under bio-inspired conditions, Angew, Chem. Int. Ed. 45 (2006) 6565–6566.

[29] H. Ueoka, The doping effects of transition elements on the PTC anomaly of semiconductive ferroelectric ceramics, Ferroelectrics 7 (1974) 351–353.

[30] A.W. Searcy, Driving force for sintering of particles with anisotropic surface energies, J. Am. Ceram. Soc. 68 (10) (1985) 267–268.

[31] D. Hennings, Recrystallization of barium titanate ceramics, Sci. Ceram. 12 (1984) 405–409.

[32] J.K. Liou, M.H. Lin, H.Y. Lu, Crystallographic facetting in sintered barium titanate, J. Am. Ceram. Soc. 85 (12) (2002) 2931–2937.

[33] Y.K. Cho, S.J. Kang, D.Y. Yoon, Dependence of grain growth and grain-boundary structure on the Ba/Ti ratio in $BaTiO_3$, J. Am. Ceram. Soc. 87 (1) (2004) 119–124.

[34] H. Schmelz, A. Meyer, The Evidence for anomalous grain growth below the eutectic temperature in $BaTiO_3$ ceramics, Ceram. Forum. Int. 59 (1982) 436–440.

[35] H. Oppolzer, H. Schmelz, Investigation of twin lamellae in $BaTiO_3$ ceramics, J. Am. Ceram. Soc. 66 (6) (1983) 444–447.